Spontaneous Nanoscale Corrugation of Ion-Eroded SiO_2: The Role of Ion-Irradiation-Enhanced Viscous Flow

Christopher C. Umbach,[1] Randall L. Headrick,[2,*] and Kee-Chul Chang[1]

[1]*Department of Materials Science and Engineering, Cornell University, Ithaca, New York 14853*
[2]*Cornell High Energy Synchrotron Source, Cornell University, Ithaca, New York 14853*

(Received 16 July 2001; published 27 November 2001)

Grazing incidence x-ray scattering was used to determine the temperature and ion-energy dependence of nanoscale corrugations that form on an amorphous SiO_2 surface eroded by Ar^+ ions. The corrugation wavelength λ^* shows a nearly linear dependence on ion energy. Between room temperature and $\sim$200 °C, λ^* depends weakly on temperature and above $\sim$200 °C it shows an Arrhenius-like increase. Ion-assisted viscous relaxation in a thin surface layer is shown to be the dominant smoothing process during erosion; the rate of viscous smoothing scales as $(\lambda^*)^{-4}$.

DOI: 10.1103/PhysRevLett.87.246104 PACS numbers: 68.35.Bs, 61.10.Kw, 81.16.Rf, 81.65.Cf

Spontaneous pattern formation during surface processing is one route to useful nanoscale textured materials. Ion-bombardment-induced surface corrugations are a notable type of such self-organization, with the potential for orienting deposited molecular films or enhancing the adhesion of metal films. Observed first on silicate glasses [1] and, in recent years, on crystals (under similar experimental conditions but with longer wavelengths [2–5]), corrugation formation depends on a balance between microscopic processes that smooth the surface, eliminating curvature gradients, and those that increase curvature, such as atom removal by ion bombardment. Surface diffusion dominates smoothing on some crystals (e.g., Si) for both thermally activated [6] and ion-enhanced diffusion [2]. Thermally activated viscous flow dominates smoothing at micron length scales on silicate glasses [7], but its influence relative to other mass transport mechanisms at submicron dimensions during ion bombardment is unknown.

In this Letter we report the use of real-time grazing-incidence small-angle x-ray scattering (RT-GISAXS) [8] to characterize the formation of corrugations on SiO_2 with wavelengths $<$200 nm, a regime where near-visible light scattering [2] cannot be applied. We explain the corrugation formation with an ion-enhanced viscous flow (IVF) model in which smoothing occurs by ion-induced viscous relaxation confined to a near-surface region of depth d; d is of the order of the ion range and of the corrugation amplitude h ($\sim$1 nm) but is much smaller than the corrugation wavelength λ^*. Without ion bombardment, the corrugations do not smooth below 800 °C, where the intrinsic viscosity of SiO_2 is high. IVF is relevant for processes using off-normal ion bombardment of disordered substrates, such as secondary ion mass spectrometry (SIMS) of device oxides.

In IVF the temperature and ion-energy dependence of λ^* are predicted more accurately than in other relevant models: (i) ion-enhanced surface diffusion (ISD) [2,9] and (ii) surface erosion smoothing (SES) in which erosion processes mimic surface diffusion [10]. The chief features of IVF follow. (1) Temperature dependence: In IVF the changes in λ^* with temperature T are attributed to a T dependence of the ion-induced viscosity η_{ion} of the thin film similar to that deduced from macroscopic stress relaxation measurements for η_{ion} of thick (2 μm) SiO_2 films [11]. We observe a weak T dependence of λ^* below 200 °C and deduce that the rearrangement of the glass network from viscous relaxation is dominated by atomic collision processes. The measured Arrhenius-like increase of λ^* above 200 °C is postulated to arise from thermally induced relaxation that aids the network rearrangements initiated by collisions. The values of λ^* predicted in SES are constant with T at low T but have magnitudes much smaller than observed. (2) Energy dependence: With the assumption in IVF that the effect of thermal excitations on the network rearrangement is independent of that of the ion-induced collision cascade, the T dependence of λ^* can be separated from its dependence on ion energy ε. The latter we predict to be a power law varying as $\varepsilon^{0.77}$. In contrast, ISD and SES suggest weaker dependencies of λ^* on ε.

The corrugations are formed on 500 nm thick SiO_2 films [conventionally wet oxidized Si(001)] in an ultrahigh vacuum chamber (5×10^{-10} torr base pressure) mounted on an x-ray beam line at the Cornell High Energy Synchrotron Source (CHESS) [12]. The bombarding Ar^+ ion beam (rastered over the sample to ensure uniform erosion of the area illuminated by the incident x rays) is incident at an angle of 45° from normal at fluxes of several $\mu A/cm^2$ with a background Ar pressure of 1×10^{-4} torr. The amount of erosion is determined *ex situ* by optical interferometry; erosion rates range from 2 Å/min to 20 Å/min, depending on ion energy and flux. Typical x-ray fluxes are 4×10^{12} photons/sec in a 10 keV beam 0.5 mm high by 2.0 mm wide. The z axis is taken normal to the sample surface, and the x axis is along the projection of the incident x-ray beam onto the sample surface. The incident x rays are near the critical angle for total external reflection. Scans are performed along the y axis with a point detector at a fixed angle 3° out of

the surface: in terms of momentum transfer, the detector scans over $\pm\Delta Q_y$ at constant Q_z and Q_x ($Q_z \approx 3$ nm^{-1}, $\Delta Q_y \approx 1$ nm$^{-1} > Q_x \approx 0.07$ nm^{-1}).

In Fig. 1 the diffuse intensity at intervals during erosion by 1.0 keV ions is plotted versus scattering vector Q_y. The ion beam is incident along the y axis, forming corrugations with a wave vector along Q_y. The single peak in diffuse intensity at time $t = 0$ arises from the initial roughness of the sample. Two peaks on either side of the central peak develop as erosion proceeds. The corrugation wavelength (inversely proportional to the separation of the peaks) remains nearly constant, but the peak intensities continue to increase and second order peaks become evident, indicating an increase in corrugation amplitude and spatial coherence. Figure 2 shows a fit of the data based on the Fourier transform [13] of an asymmetric sawtooth surface profile where the sidewall with positive slope (i.e., more parallel to the ion beam) has a slope $\sim 1.5°$ greater in absolute value than the negatively sloped sidewall. The corrugation amplitudes (~ 10 Å) and wavelengths deduced from the x-ray scattering are consistent with atomic force microscope (AFM) measurements of surfaces sputtered at all the ion energies studied (0.5 to 2 keV); the inset of Fig. 2 is an *ex situ* AFM image of the surface acquired after the x-ray measurements. The rate of amplitude increase does vary with ion flux f, but the value of λ^* is insensitive to f within the experimentally accessible factor of three range in f.

Before describing our measurement of the dependence of λ^* on ε and T, we turn first to the quantitative predictions within the IVF model. During corrugation formation curvature gradients increase because of a morphological instability by which regions of negative surface curvature (pits) erode faster than regions of positive curvature (bumps) [14]; this is the only curvature-gradient increasing process considered relevant for amorphous SiO_2, although different such processes may occur on crystals. Curvature-dependent smoothing by which material is transported from regions of high curvature to regions of low curvature opposes increases in curvature; for disordered materials viscous flow must be considered in addition to surface and bulk diffusion. Bradley and Harper (BH) predicted that, for surface diffusion, a stable sinusoidal surface of constant wavelength develops during off-normal sputtering [15]. The surface amplitude $h(x,t)$ as a function of spatial coordinate x (in the average plane of the eroding surface) and time t is expected to be $h(x,t) = h_0 \cos(qx - \Omega t)e^{rt}$. Here h_0 is the initial amplitude, q is $2\pi/\lambda^*$, Ω/q is a lateral phase velocity, and r is an exponential growth rate. If the corrugation wave vector q has a component along the ion beam direction (as is the case here), $\Omega \neq 0$ because positive and negative slopes erode at different rates, translating the sinusoid laterally [16].

Mayer, Chason, and Howard (MCH) modified the BH model to derive an ion-induced surface diffusivity of SiO_2 consistent with the observation of 300 Å wavelength corrugations after sputtering with 1 keV Xe^+ ions [17]. MCH included in the growth rate r terms due both to smoothing by viscous flow and by ion-enhanced surface diffusion. The viscous term is found by solving the two-dimensional Navier-Stokes equations with boundary conditions for a sinusoid (attempting to describe viscous smoothing using local spatial derivatives [18] overlooks the nonlocal character of viscous flow). Two limiting cases are relevant. In the first limit (used by MCH), fluxes extend into the

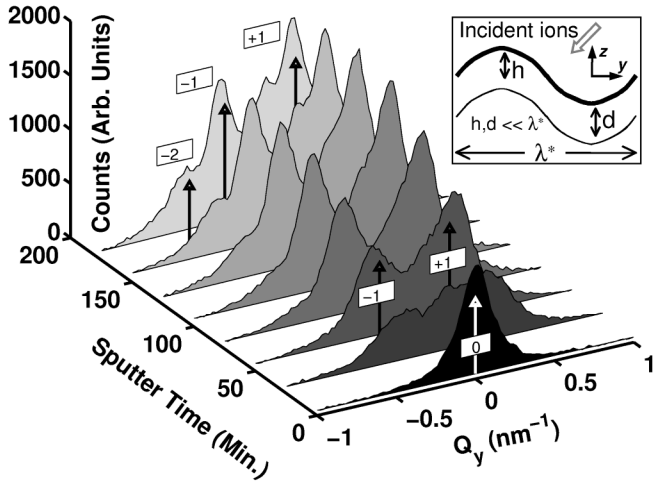

FIG. 1. Diffuse intensity from SiO_2 sputtered by 1 keV Ar^+ versus time and x-ray scattering vector Q_y. The arrows mark orders of the corrugation periodicity as determined by the fit to the final line shape (see Fig. 2). Inset: Geometry of incident ions and corrugation wavelength λ. The near-surface viscosity is reduced in a region of thickness d, comparable to the ion range and the corrugation amplitude h. The vertical scale of the inset is enhanced relative to that of the horizontal.

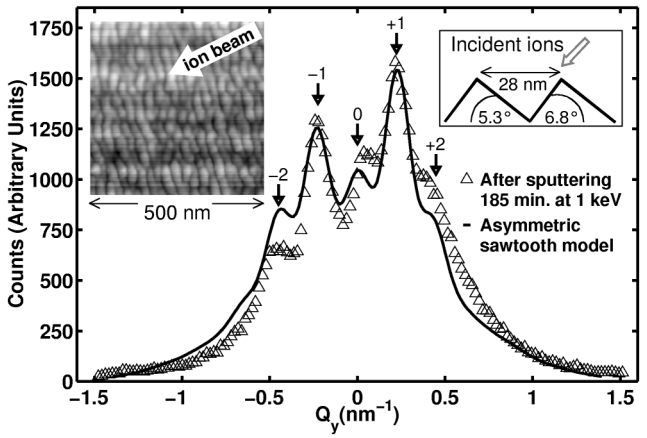

FIG. 2. Diffuse scattering from sample of Fig. 1 after 185 min of sputtering. The data are fit by an asymmetric sawtooth surface with a wavelength of 28 nm; arrows indicate orders of corrugation periodicity. Left inset: AFM image taken *ex situ* after the x-ray measurements showing the projected ion beam direction. Right inset: model surface profile.

bulk a distance comparable to λ. In the second limit (proposed here), viscous flow is confined to a surface layer of thickness $d \ll \lambda$. Smoothing by bulk viscous flow [19] contributes a term $-F_b q$ to the rate of growth; smoothing by surface-confined viscous flow [20] contributes a term $-F_s d^3 q^4$. Here $F_b(F_s)$ is proportional to γ/η_b (γ/η_s), where η_b and η_s are the bulk and surface viscosities, respectively, and γ is the surface tension, assumed to be constant and isotropic.

The growth rate r_b for bulk viscous relaxation [17] is $r_b = Sq^2 - F_b q - Bq^4$, where S is a prefactor related to the curvature-dependent erosion rate and B is proportional to the surface diffusivity. The growth rate r_s for surface viscous relaxation is $r_s = Sq^2 - F_s d^3 q^4 - Bq^4$. Differentiating r_b or r_s with respect to q will determine if there is a corrugation wave vector q^* for which r is positive and maximum; the corrugation with wave vector q^* will grow faster than all others. For bulk viscous relaxation with $B = 0$, no such wavelength selection occurs. When either surface diffusion or surface viscous relaxation dominates, then there exists a q^* for which r_b or r_s is maximized.

Ion-induced viscous flow occurs in a surface layer with a depth on the order of the ion range (<50 Å in the present experiments) and the limit of surface-confined viscous flow can be applied. As explained below in our discussion of ISD models, surface diffusion is taken as negligible; with $B = 0$, r_s is maximum at $\lambda^*_{\mathrm{IVF}} = 2\pi(2F_s d^3/S)^{1/2}$. For ions incident with angle θ measured from the normal, $S = (fa/n)Y(\theta)\Gamma(\theta)$, where a is the average depth of energy deposition by the ions, n is the atomic density, $Y(\theta)$ is the sputter rate per ion, and $\Gamma(\theta)$ is a parameter related to the curvature dependence of the erosion rate. Following previous work [17] we write $\eta_s = \eta_r/f$, where $1/\eta_r$ is a flux-independent measure of the viscous *relaxation* per ion; $1/\eta_r$ varies with ion energy as ε^α. From Table 1 in Ref. [17], which gives the rates at which sputter-induced corrugations smooth due to H^+ and He^+ bombardment, a value of $\alpha \approx 1$ can be deduced [21]. Equating the depth of energy deposition, a, to the depth of the reduced viscosity layer, d, gives

$$\lambda^*_{\mathrm{IVF}} = 2\pi d[2\gamma n/(\Gamma(\theta)Y(\theta)\eta_r)]^{1/2}. \qquad (1)$$

Here λ^*_{IVF} is independent of f, which is consistent with our observations. The ion-collision simulator TRIM [22] indicates that d and $Y(\theta)$ vary as ε^δ, with $\delta \approx 0.55$. $\Gamma(\theta)$ depends very weakly on ε. Hence $\lambda^*_{\mathrm{IVF}} \propto \varepsilon^{\mathrm{p}}$ where $p = \alpha/2 + 0.27$, giving $p = 0.77$ for $\alpha \approx 1$.

Figure 3 shows the observed dependence of λ^* on inverse temperature $1/T$ for three different ion energies. Samples were preannealed to 800 °C and then sputtered at temperature until a well-defined λ^* developed. Writing $1/\eta_r \propto \varepsilon^\alpha[\exp(-E/k_B T) + \omega]$ to represent the separate ε and T dependence of $1/\eta_r$, the data are fit with Eq. (1) written as $\lambda^*_{\mathrm{IVF}}(\varepsilon, T) = H(\varepsilon)W(T)$, where $H(\varepsilon) = c\varepsilon^{\mathrm{p}}$ and $W(T) = [\exp(-E/k_B T) + \omega]^{1/2}$. E is a barrier for the thermally activated rearrangement of the network, ω represents the fraction of the ion-induced viscous relaxation that is T independent, ε^p represents the ε dependence of $d(Y(\theta)\eta_r)^{-1/2}$, and c is a constant. Values of $E = 0.4$ eV and $p = 0.85$ are found in a nonlinear least squares fit (the solid lines in Fig. 3). To exhibit the power law dependence on ε alone, in the inset of Fig. 3 each measured $\lambda^*(\varepsilon, T)$ scaled for its fitted temperature dependence is plotted, where $\lambda^*_{\mathrm{scaled}}$ is given by $\lambda^*(\varepsilon, T)[\omega^{1/2}/W(T)]$. Also plotted are fits of $\lambda^*_{\mathrm{scaled}}$ to ε^p for $p = 0.5$, 0.77, 0.85, and 1.0.

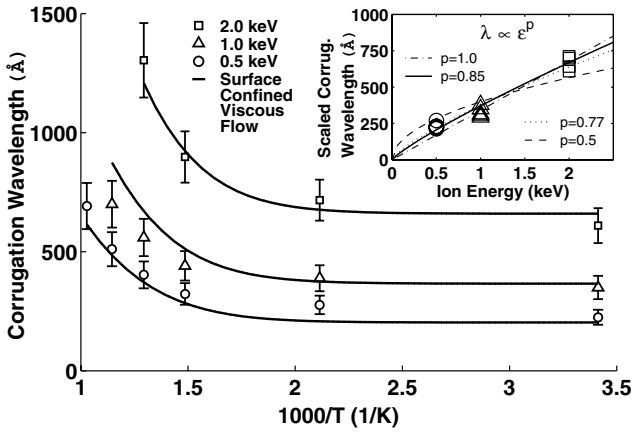

FIG. 3. Corrugation wavelength λ^* as a function of inverse temperature for different ion energies. Solid line: fit to IVF model. Inset: λ^* scaled for temperature dependence versus ion energy ε. The measurement error is comparable to the height of the symbol. Fits to different power law exponents are shown.

The fitted power law dependence of $p = 0.85$ and that of the IVF model ($p = 0.77$) are indistinguishable within experimental error. A similar f independence and ε^p dependence ($p = 0.8$) of λ^* were reported for corrugations formed by off-normal sputtering of crystalline Si with O_2^+ ions (1 to 9 keV) in a SIMS instrument [9]. This consistency with the IVF model should occur for any material with a disordered surface layer that relaxes viscously [23], arising in Ref. [9] from a high surface oxygen concentration.

The value of $E = 0.4$ eV likely represents an average activation energy associated with collective motion of network defects. The presence of low-energy ($E < 0.75$ eV) ion-induced defect structures that contribute to structural rearrangements during annealing has been deduced from measurements of the relaxation of stress in thick SiO_2 films *after* MeV ion irradiation [24]. Because MeV ions lose a significant amount of energy via electronic excitations (unlike the keV ions used here) in addition to the energy lost to nuclear collisions, the distribution of network defects is not the same for the two ion-energy regimes, although similar defects exist in both cases. Thick-film measurements *during* MeV irradiation have determined that η_r is thermally activated above 130 °C and constant below

[12], supporting the assumption in IVF of a temperature-independent contribution to the ion-induced viscous relaxation.

The dominance of ion-enhanced viscous flow over ion-enhanced surface diffusion is justified by considering two representative ISD models that are applicable to disordered materials and that predict an f-independent λ^*. (1) ISD(1): When diffusion occurs in a thin, ion-damaged surface layer with a thickness on the order of the ion range, it is predicted that $\lambda^*_{\mathrm{ISD}} \propto \varepsilon^{0.5-\delta}$, where the sputter yield $Y(\theta)$ varies as ε^{δ} (Eq. 10 in Ref. [9]). Using $\delta = 0.55$ (appropriate for our experiments) λ^*_{ISD} varies weakly with ε in ISD(1). (2) ISD(2): For molecules diffusing only on the surface and recombining with surface traps, $\lambda^*_{\mathrm{ISD}} \propto [l^2_{\mathrm{trap}}/dY(\theta)]^{1/2}$ [2]; l_{trap} is the length between traps and is independent of f. We extend ISD(2) by considering the dependence of l_{trap} on ε. For a trap concentration c_{trap} determined by intrinsic defects, l_{trap} is independent of ε; if c_{trap} increases with sputter damage (and hence with ε), l_{trap} should decrease with ε. Hence $\lambda^*_{\mathrm{ISD}} \propto \varepsilon^{-p}$, where $p \geq 0.5$. Despite the agreement with our observation of a f-independent λ^*, in both ISD(1) and ISD(2) the dependence of λ^* on ε is different than that observed, suggesting smoothing by ion-enhanced surface diffusion is negligible in our experiments.

Smoothing by erosion is treated in the SES model, where a smoothing term in the exponential growth rate r varying as q^4 (analogous to surface diffusion and surface viscous relaxation) arises from the sputter process itself [10]. As measured at low T, SES predicts a dominant wavelength λ^*_{SES} independent of T and f. However, the predicted values of λ^*_{SES} are of the order of the width of the region where the ion deposits energy, which varies as $\varepsilon^{0.5}$ at the experimental energies and is $\sim$10 times smaller than our measured values of λ^*, suggesting that SES alone cannot account for the observed low-T behavior.

In summary, we have shown that smoothing by surface-confined ion-induced viscous flow during off-normal ion etching leads to corrugation formation. Our model provides better quantitative agreement with the data presented here than models based on smoothing by surface diffusion or surface erosion. The microscopic processes involved in ion-induced viscous relaxation could be elucidated by molecular dynamics simulations similar to those used to model changes in glass structure due to radioactivity-induced atomic collisions [25].

We acknowledge the advice and encouragement of J. M. Blakely; the scientific insights of E. Chason, D. Cahill, L. Barabasi, M. Rauscher, and J. Sethna; and the experimental assistance of A. Couture, E. Butler, and O. Malis. This work was supported by the National Science Foundation through Grant No. DMR-96-32275 to the Cornell Center for Materials Research and Grant No. DMR-97-13424 to CHESS.

*Current address: Department of Physics, University of Vermont, Burlington, VT 05405.

[1] M. Navez, C. Sella, and D. Chaperot, Compt. Rend. J. Phys. **254**, 240 (1962).
[2] J. Erlebacher *et al.,* Phys. Rev. Lett. **82**, 2330 (1999).
[3] E. Chason *et al.,* Phys. Rev. Lett. **72**, 3040 (1994).
[4] S. W. MacLaren *et al.,* J. Vac. Sci. Technol. A **10**, 468 (1992).
[5] S. Rusponi, C. Boragno, and U. Valbusa, Phys. Rev. Lett. **78**, 2795 (1997).
[6] M. E. Keeffe, C. C. Umbach, and J. M. Blakely, J. Phys. Chem. **55**, 965 (1994).
[7] D. C. Cassidy and N. A. Gjostein, J. Am. Ceram. Soc. **53**, 161 (1970).
[8] J. R. Levine, J. B. Cohen, and Y. W. Chung, Surf. Sci. **248**, 215 (1991).
[9] J. J. Vajo, R. E. Doty, and E.-H. Cirlin, J. Vac. Sci. Technol. A **14**, 2709 (1996).
[10] M. A. Makeev and A. L. Barabasi, Appl. Phys. Lett. **71**, 2800 (1997).
[11] M. L. Brongersma, E. Snoeks, and A. Polman, Appl. Phys. Lett. **71**, 1628 (1997).
[12] R. L. Headrick *et al.,* Phys. Rev. B **54**, 14 686 (1996).
[13] M. Yoon *et al.,* Surf. Sci. **411**, 70 (1998).
[14] P. Sigmund, J. Mater. Sci. **8**, 1545 (1973).
[15] R. M. Bradley and J. M. E. Harper, J. Vac. Sci. Technol. A **6**, 2390 (1987).
[16] In BH erosion and smoothing are linear in the surface spatial derivatives; numerical analysis indicates that nonlinear terms of the form $(\frac{\partial h}{\partial x})(\frac{\partial^2 h}{\partial x^2})$ produce asymmetric features, suggesting an origin for the observed asymmetric surface profile, cf. M. A. Makeev, C. Cuerno, and A. L. Barabasi (unpublished) available at http://xxx.lanl.gov/abs/cond-mat/0007354.
[17] T. M. Mayer, E. Chason, and A. J. Howard, J. Appl. Phys. **76**, 1633 (1994).
[18] G. Carter, Phys. Rev. B **59**, 1669 (1999).
[19] S. Pai, in *Viscous Flow Theory, Laminar Flow* (Van Nostrand, Princeton, 1956), Vol. I, p. 129; W. W. Mullins, J. Appl. Phys. **30**, 77 (1959).
[20] S. E. Orchard, Appl. Sci. Res. **11A**, 451 (1962).
[21] Since the light ion range approaches $\sim\lambda^*/2$, the assumption [17] of *bulk* flow to find η_r from surface smoothing, giving $\alpha \approx 1$, is reasonable. Macroscopic curvature relaxation at MeV ion energies gives $\alpha \approx 0.5$, cf. E. Snoeks *et al.,* J. Appl. Phys. **78**, 4723 (1995).
[22] J. F. Ziegler, J. P. Biersack, and U. Littmark, *Stopping and Range of Ions in Solids* (Pergamon Press, New York, 1985).
[23] Corrugations form if viscous smoothing varies as q^n for $n > 2$. As d/λ increases, values of $n < 4$ become appropriate [20]. For example, when $n \approx 3$, by dimensional arguments the smoothing is $-F_s d^2 q^3$, predicting $\lambda^*_{\mathrm{IVF}} \propto \varepsilon^p$ where $p = \alpha$,
[24] T. van Dillen *et al.,* Nucl. Instrum. Methods Phys. Res., Sect. B **148**, 221 (1999).
[25] J. M. Delaye and D. Ghaleb, J. Nucl. Mater. **244**, 22 (1997).